

The non-isothermal devitrification of glasses in the CaO·4GeO₂–BaO·4GeO₂ composition range

M. Catauro^{*}, S. Gargano, G. Laudisio

Department of Materials and Production Engineering, University Federico II Piazzale Tecchio, 80125 Napoli, Italy

Received 12 December 1999; accepted 12 February 2000

Abstract

The effect of replacing CaO by BaO on the glass transition temperature and on devitrification behaviour in a series of glasses in the calcium tetragermanate–barium tetragermanate composition range has been studied by differential thermal analysis (DTA), X-ray diffraction (XRD) and Fourier-transform infrared (FTIR) spectra. A similar GeO₄/GeO₆ molar ratio was found in all the glasses of the series. The progressive replacement of CaO by BaO caused a decrease in the glass transition temperature. All the glasses studied exhibited internal crystal nucleation. The crystallizing phases were identified as CaGe₄O₉ and BaGe₄O₉. No solid solutions occurred in the glass containing both CaO and BaO. The effect of the specific surface of the glass samples on devitrification processes has also been studied. © 2000 Elsevier Science B.V. All rights reserved.

Keywords: Devitrification; Glass transition temperature; Alkaline earth germanate

1. Introduction

The properties of binary M₂O–GeO₂ and MO–GeO₂ glasses have been studied extensively [1–6]. Phase equilibria in the binary germanate system have been also reported [7]. On the other hand, very little is known about ternary germanate glasses. This paper is part of a research program with the aim of filling this gap.

In previous papers [8–10], the effect on glass transition temperature and devitrification behavior of the progressive substitution of an alkaline oxide M₂O by another M'₂O oxide in tetragermanate glasses were discussed. The substitution of M₂O by M'₂O causes the value of the glass transition temperature to go through

a minimum at molar ratio M₂O/M'₂O=1 according to the 'mixed alkali effect'. The structures of all the studied glasses contain GeO₄ and GeO₆ groups in about the same molar ratio. In lithium–sodium tetragermanate glasses, a ternary compound LiNaGe₄O₉ was found among the crystallizing phases [8]. The stability of lithium–potassium tetragermanate glasses increases with the increase in the difference between crystallizing phases and mother glass composition [9]. In sodium–potassium tetragermanate glasses, solid solutions between Na₄Ge₉O₂₀ and K₄Ge₉O₂₀ crystallize [10]. In strontium–barium tetragermanate glasses, a solid solution between SrGe₄O₉ and BaGe₄O₉ was found to crystallize in glass containing both SrO and BaO [11]. The devitrification behavior of ternary tetragermanate glasses containing Ba⁺⁺ and Pb⁺⁺ ions in 3/1, 1/1 and 1/3 molar ratios has also been studied [12]. Glasses with 3/1 and 1/1 Ba⁺⁺

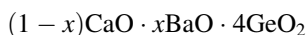
^{*} Corresponding author. Tel.: +39-81-758-23;
fax: +39-81-758-2595.

Pb^{++} molar ratios are phase-separated and devitrified in two steps. Bulk crystallization of BaGe_4O_9 is followed at higher temperatures by GeO_2 crystals growth on the surface of the samples. The glass with $1/3 \text{ Ba}^{++}/\text{Pb}^{++}$ molar ratio devitrifies into a solid solution of BaGe_4O_9 and PbGe_4O_9 crystals.

In the present work, the effect of a progressive replacement of CaO by BaO , on the structure, the glass transition temperature and the devitrification behavior of tetragermanate glasses were studied by Fourier-transform infrared spectroscopy (FTIR), differential thermal analysis (DTA) and X-ray diffraction (XRD).

2. Experimental

The glass compositions are expressed by the general formula



with $x=0.00; 0.25; 0.50; 0.75; 1.00$. In the course of the paper, each glass is named by the corresponding x value. The glasses were prepared by mixing appropriate quantities of ultra pure calcium carbonate (Aldrich), barium carbonate (Aldrich) and germanium oxide (Heraeus) in a batch sized to yield 3 g of glass. The glasses were melted in an uncovered Pt crucible in an electric oven. The crucible containing the glass was weighed both before and after the glass was removed. The weight of the glass agreed with that anticipated from the batch calculation. This result indicates that the actual glass composition is close to that based on the glass batch. The melts were quenched by plunging the bottom of the crucible into cold water. Although this resulted in fracture of the glass, for all the compositions, pieces of transparent glass of size sufficient for the experimental measurements were obtained by this technique.

FTIR absorption spectra were recorded in the $4000\text{--}400 \text{ cm}^{-1}$ range using a Mattson 5020 system, equipped with a deuterated triglycine sulfate with potassium bromide windows (DTGS KBr) detector. A spectral resolution of 2 cm^{-1} was chosen. Each test sample was mixed with KBr (1 wt.% of former) in an agate mortar, and then pressed into 200 mg pellets of 13 mm diameter. The spectrum for each sample represents an average of 20 scans, which were normalized

to the spectrum of the blank KBr pellet. The FTIR spectra have been analyzed by a Mattson software (FIRST Macros).

DTA curves were recorded in air at a heating rate of $10^\circ\text{C min}^{-1}$ on bulk or fine powdered ($<45 \mu\text{m}$) specimens (about 50 mg) from room temperature to 900°C . A Netzsch thermoanalyser High Temperature DSC 404 was used with Al_2O_3 as reference material. The experimental error in DTA temperature is $\pm 1^\circ\text{C}$. The DTA curves have been elaborated by a Netzsch software.

The amorphous nature of the glasses and the identification of the phases crystallizing in the glass during the DTA runs were ascertained by XRD using a Philips diffractometer. Powders of each glass sample were scanned from $2\Theta=5\text{--}60^\circ$ using $\text{Cu K}\alpha$ radiation.

3. Results and discussion

Fig. 1 shows the infrared transmission spectra of the as-quenched glasses in the $400\text{--}1200 \text{ cm}^{-1}$ range where the $\text{Ge}\text{--}\text{O}\text{--}\text{Ge}$ and $\text{O}\text{--}\text{Ge}\text{--}\text{O}$ stretching and deformation modes are active. The two strongest absorption peaks lie at about 750 and 570 cm^{-1} .

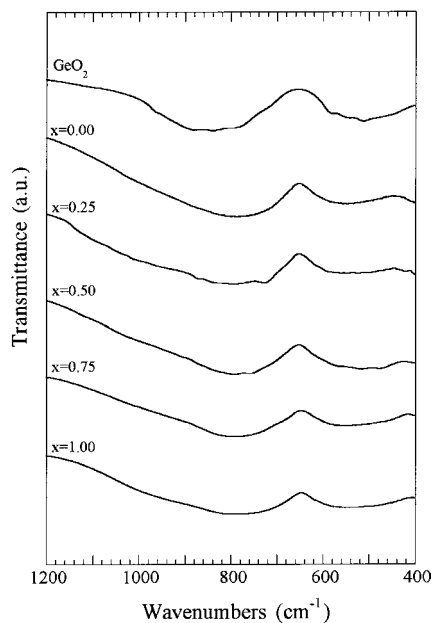


Fig. 1. FTIR transmittance spectra for glasses of composition $(1-x)\text{CaO} \cdot x\text{BaO} \cdot 4\text{GeO}_2$.

Table 1
DTA and IR data for glasses of composition $(1-x)\text{CaO}\cdot x\text{BaO}\cdot 4\text{GeO}_2^a$

Glasses	T_g (°C)	T_{p1} (°C)	T_{p2} (°C)	ν_1 (cm^{-1})	ν_2 (cm^{-1})
$x=0.00$	688	730 [707]	800	756	577
$x=0.25$	674	718 [718]	799	748	575
$x=0.50$	665	702 [698]		747	569
$x=0.75$	659	688 [690]		754	576
$x=1.00$	638	677 [675]		754	569

^a T_g : glass transition temperatures; T_p : DTA peak temperatures of bulk samples [in square brackets, those of powdered samples]; ν_1 and ν_2 : frequencies of the two strongest intensity bands in crystallized samples.

From previous studies [4], it is known that, in the infrared spectra of hexagonal and vitreous GeO_2 , in which the coordination number of germanium is 4, the absorption band, due to the Ge–O–Ge stretching, lies at 878 cm^{-1} , while in tetragonal GeO_2 , in which germanium assumes six-fold coordination, this band occurs at 688 cm^{-1} . In alkali germanate, the coordination number of Ge atoms changes from 4 to 6 with the addition of alkali oxide to GeO_2 glass and this band progressively shifts towards lower wavenumber values [4].

The spectra of Fig. 1 exhibit almost the same shift of this band as shown in Table 1. This result suggests a similar $\text{GeO}_4/\text{GeO}_6$ molar ratio in all the glasses of the series. The absorption band at about 550 cm^{-1} may be related to the mixed stretching–bending vibrations of GeO_4 tetrahedra [13].

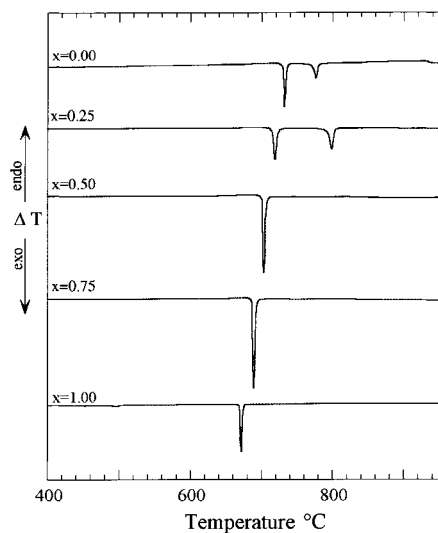


Fig. 2. DTA curves recorded at $10^\circ\text{C min}^{-1}$ for glasses of composition $(1-x)\text{CaO}\cdot x\text{BaO}\cdot 4\text{GeO}_2$.

Fig. 2 shows the DTA curves of the five as-quenched glasses recorded on bulk samples. A slope change followed by an exothermic peak occurs on all curves. The slope change may be attributed to the glass transition. In this work, the extrapolated onset of the slope change was taken (Fig. 3) as the glass transition temperature, T_g . The values of T_g for the five investigated glasses are reported in Table 1.

According to Ray [14], the effect of any cation on T_g is related to the following factors: (i) reduction in the density of covalent cross-linking; (ii) change in oxygen density of the network; (iii) number and strength of the cross-links between oxygen and the cation. In the glasses studied, the O/Ge ratio is constant (i.e. O/Ge=2.25) and the $\text{GeO}_4/\text{GeO}_6$ molar ratio is the same, therefore the cross-link density does not change. The strength and the number of the cross-links between oxygen and the cations are related to the coordination number and to the radius and of the cations. The coordination number is 8 for both cations. The M–O strength is reduced as a result of the larger

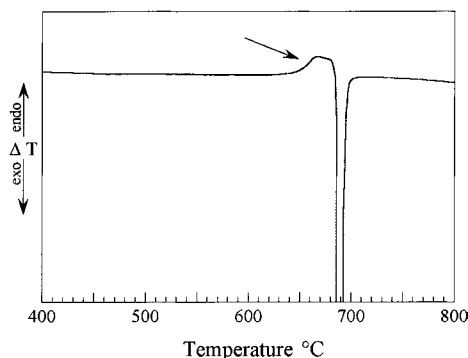


Fig. 3. DTA curve of the term $x=0.00$ shown on expanded ordinate scale to well display the slope change attributed to the glass transition.

radii of Ba^{++} (0.143 nm) compared to Ca^{++} (0.099 nm). Therefore, the progressive replacement of Ca^{++} by Ba^{++} causes the decrease in the glass transition temperature.

Nucleation in glass-forming systems can occur either in the volume or on the surface of the sample. In practice, surface crystal nucleation occurs more easily and is observed in most compositions. To achieve internal crystal nucleation, it is often necessary to add nucleating agents. However, certain glass systems nucleate internally without such additions. The total number of nuclei, N , per unit volume is the sum of surface nuclei, N_s , of homogeneous bulk nuclei N_b formed during the DTA run and heterogeneous bulk nuclei N_c [15]. The values of N_s , N_b and N_c are proportional to the specific surface area of the samples, the reciprocal of the DTA heating rate and the amount of nucleating agent, respectively. The higher the number of N , the lower the temperature of the DTA crystallization peak [16]. Moreover, the shape of the DTA crystallization peak is strongly affected by the crystallization mechanism [17], with surface and bulk crystallization corresponding to broad and sharp peaks, respectively.

In the glasses studied, no nucleating agent was added ($N_c=0$). The sharp shape of the crystallization peaks on the DTA curves, carried out on bulk samples (low specific surface area) (Fig. 2) suggests that, in all glasses studied, internal crystal nucleation is dominant, $N_b \gg N_s$. To confirm this hypothesis, DTA curves were also recorded on very fine powdered samples. No appreciable differences in the temperature, T_p (see Table 1) and the shape of the crystallization peak were found. Taking into account the great increase in the number of surface nuclei due to the high specific surface area of the very fine powdered samples, this result indicates that the specific surface area of the samples has no influence on the devitrification process of these glasses and surface crystallization compared to bulk nucleation can be neglected.

To ascertain the amorphous nature of the glasses and to identify the phases crystallizing during the DTA runs, XRD measurements were carried out on the as-quenched glasses and on samples subjected to a DTA run from room temperature to the temperature of each DTA exo-peak.

The XRD patterns of the as-quenched glasses show broad humps characteristic of their amorphous state.

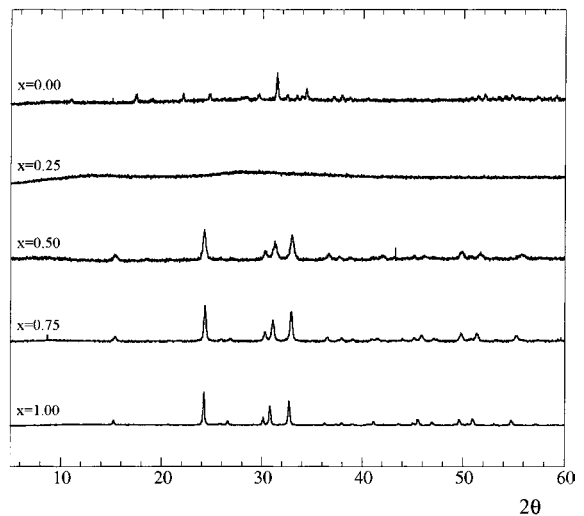


Fig. 4. XRD patterns for glasses of composition $(1-x)\text{CaO} \cdot x\text{BaO} \cdot 4\text{GeO}_2$ heated until the temperature of the first DTA exo-peak.

The XRD patterns of samples of the glasses heated to the temperature of the first DTA peak except the term $x=0.25$ exhibit (Fig. 4) several sharp reflections that were all assigned to CaGe_4O_9 (JCPDS file 14-515) and BaGe_4O_9 (JCPDS file 13-295) crystals.

The diffractogram of the term $x=0.25$ has broad humps characteristic of the amorphous state. This result and the glassy look of the sample after the heat treatment, in spite of the strong thermal effect on the DTA curve, suggest the precipitation of a high number of microcrystallites dispersed in a non-crystalline matrix.

The diffractograms obtained for the terms $x=0.00$ and $x=0.25$ heated above both the crystallization exothermic peaks (Fig. 5) exhibit a high number of sharp lines that all correspond to CaGe_4O_9 crystals (JCPDS file 14-515).

For a range of simple substitutional solid solutions to form, there are certain requirements that must be met. First, the ions that replace each other must have the same charge. Second, the ions that are replacing each other must be fairly similar in size. From a review of the experimental result on metal alloy formation, it has been suggested that a difference of 15% in the radii of the metal atoms that replace each other is the most that can be tolerated if a substantial range of substitutional solid solutions is to form. In considering

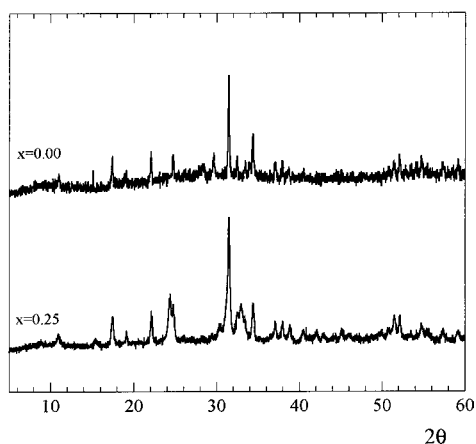


Fig. 5. XRD patterns of the term $x=0.00$ and $x=0.25$ heated until the temperature of the second DTA exo-peak.

whether or not solid solutions form, an important factor is the crystal structure of the two end members. In the systems that exhibit complete ranges of solid solution, it is clearly essential that the two end members be isostructural. The reverse is not necessarily true, however, and just because two phase are isostructural, it does not follow that they will form solid solutions with each other.

The XRD patterns of the crystallizing phases in the terms of the series shown in Fig. 4 suggest that the two phases are isostructural but the solid solutions do not form.

Table 2
Crystallizing phase $(1-x)\text{CaO}\cdot x\text{BaO}\cdot 4\text{GeO}_2^a$

$(1-x)\text{CaO}\cdot x\text{BaO}\cdot 4\text{GeO}_2$	Crystallizing phase
$x=0.00$	CaGe_4O_9
$x=0.25$	CaGe_4O_9
$x=0.50$	CaGe_4O_9 $\text{BaGe}_4\text{O}_9(\text{tc})$
$x=0.75$	BaGe_4O_9
$x=1.00$	BaG_4O_9

^a tc: trace.

The crystallizing phases during the DTA runs are reported in the Table 2.

4. Conclusions

From the experimental results, the following conclusions can be drawn:

1. The structures of the devitrified glasses contain GeO_4 and GeO_6 in the same molar ratio.
2. The progressive replacement of CaO by BaO causes a progressive decrease in the glass transition temperature.
3. All glasses exhibit internal crystal nucleation.
4. The crystallizing phases are CaGe_4O_9 and BaGe_4O_9 . No solid solution were found.

References

- [1] K.S. Evstropiev, A.O. Ivanov, in: F.R. Matson, G.E. Rindone (Eds.), *Advances in Glass Technology*, Part 2, Plenum Press, New York, 1963, p. 79.
- [2] M.K. Murty, J. Ip, *Nature (London)* 201 (1964) 3285.
- [3] J.E. Shelby, *J. Am. Ceram. Soc.* 57 (1974) 436.
- [4] M.K. Murthy, E.M. Kirby, *Phys. Chem. Glasses* 5 (1964) 144.
- [5] S. Sakka, K. Kamiya, *J. Non-Cryst. Solids* 49 (1982) 103.
- [6] H. Verweij, J.H.J.M. Buster, *J. Non-Cryst. Solids* 34 (1979) 81.
- [7] E.M. Levin, C.R. Robins, H.C. McMurdie, *Phase Diagrams for Ceramists*, American Ceramic Society, Columbus, OH, 1964, p. 93.
- [8] M. Catauro, A. Aronne, P. Pernice, A. Marotta, *J. Mater. Sci. Lett.* 15 (1996) 817.
- [9] G. Laudisio, M. Catauro, *J. Eur. Ceram. Soc.* 18 (1998) 359.
- [10] G. Laudisio, M. Catauro, *Mater. Chem. Phys.* 51 (1997) 54.
- [11] M. Catauro, G. Laudisio, *J. Thermal Anal.* in press.
- [12] G. Laudisio, M. Catauro, *Phys. Chem. Glasses* 39 (1998) 62.
- [13] K.E. Lipinska-Kalita, *J. Non-Cryst. Solids* 119 (1990) 41.
- [14] N.H. Ray, *J. Non-Cryst. Solids* 15 (1974) 423.
- [15] A. Marotta, A. Buri, F. Branda, *Thermochim. Acta* 40 (1980) 397.
- [16] A. Marotta, A. Buri, F. Branda, *J. Mater. Sci.* 16 (1981) 341.
- [17] W.W. Wendlandt, in: *Thermal Analysis*, Wiley, 1986, p. 448.